Chemico-Biological Interactions 221 (2014) 13–23

Contents lists available at ScienceDirect

Chemico-Biological Interactions

journal homepage: www.elsevier.com/locate/chembioint

The mechanism of honokiol-induced intracellular Ca^{2+} rises and apoptosis in human glioblastoma cells

Wei-Zhe Liang [a], Chiang-Ting Chou [b,c], Hong-Tai Chang [d], Jin-Shiung Cheng [e], Daih-Huang Kuo [f], Kuang-Chung Ko [g], Ni-Na Chiang [h], Ru-Fang Wu [i], Pochuen Shieh [f], Chung-Ren Jan [a,*]

[a] Department of Medical Education and Research, Kaohsiung Veterans General Hospital, Kaohsiung 813, Taiwan, ROC
[b] Department of Nursing, Division of Basic Medical Sciences, Chang Gung University of Science and Technology, Chia-Yi 613, Taiwan, ROC
[c] Chronic Diseases and Health Promotion Research Center, Chang Gung University of Science and Technology, Chia-Yi 613, Taiwan, ROC
[d] Department of Surgery, Kaohsiung Veterans General Hospital, Kaohsiung 813, Taiwan, ROC
[e] Department of Medicine, Kaohsiung Veterans General Hospital, Kaohsiung 813, Taiwan, ROC
[f] Department of Pharmacy, Tajen University, Pingtung 907, Taiwan, ROC
[g] Department of Gastroenterology, Kaohsiung Veterans General Hospital-Pingtung Branch 912, Taiwan, ROC
[h] Department of Pharmacy, Kaohsiung Veterans General Hospital-Pingtung Branch 912, Taiwan, ROC
[i] Department of Pharmacy, Kaohsiung Municipal Kai-Syuan Psychiatric Hospital, Kaohsiung 802, Taiwan, ROC

ARTICLE INFO

Article history:
Received 29 November 2013
Received in revised form 15 July 2014
Accepted 25 July 2014
Available online 7 August 2014

Keywords:
Honokiol
Human glioblastoma cells
Ca^{2+}
Apoptosis
Mitochondrial membrane potential

ABSTRACT

Honokiol, an active constituent of oriental medicinal herb *Magnolia officinalis*, caused Ca^{2+} mobilization and apoptosis in different cancer cells. *In vivo*, honokiol crossed the blood–brain or –cerebrospinal fluid barrier, suggesting that it may be an effective drug for the treatment of brain tumors, including glioblastoma. This study examined the effect of honokiol on intracellular Ca^{2+} concentration ($[Ca^{2+}]_i$) and apoptosis in DBTRG-05MG human glioblastoma cells. Honokiol concentration-dependently induced a $[Ca^{2+}]_i$ rise. The signal was decreased partially by removal of extracellular Ca^{2+}. Honokiol-triggered $[Ca^{2+}]_i$ rise was not suppressed by store-operated Ca^{2+} channel blockers (nifedipine, econazole, SK&F96365) and the protein kinase C (PKC) activator phorbol 12-myristate 13 acetate (PMA), but was inhibited by the PKC inhibitor GF109203X. GF109203X-induced inhibition was not altered by removal of extracellular Ca^{2+}. In Ca^{2+}-free medium, pretreatment with the endoplasmic reticulum Ca^{2+} pump inhibitor thapsigargin (TG) or 2,5-di-tert-butylhydroquinone (BHQ) abolished honokiol-induced $[Ca^{2+}]_i$ rise. Conversely, incubation with honokiol abolished TG or BHQ-induced $[Ca^{2+}]_i$ rise. Inhibition of phospholipase C (PLC) with U73122 abolished honokiol-induced $[Ca^{2+}]_i$ rise. Honokiol (20–80 μM) reduced the cell viability, which was not reversed by prechelating cytosolic Ca^{2+} with BAPTA-AM (1,2-bis(2-aminophenoxy)ethane-N,N,N′,N′-tetraacetic acid-acetoxymethyl ester). Honokiol (20–60 μM) enhanced reactive oxygen species (ROS) production, decreased mitochondrial membrane potential, released cytochrome c, and activated caspase-9/caspase-3. Together, honokiol induced a $[Ca^{2+}]_i$ rise by inducing PLC-dependent Ca^{2+} release from the endoplasmic reticulum and Ca^{2+} entry via PKC-dependent, non store-operated Ca^{2+} channels. Moreover, honokiol activated the mitochondrial pathway of apoptosis in DBTRG-05MG human glioblastoma cells.

1. Introduction

Magnoliae officinalis is a traditional Chinese medicine. The root and bark of *M. officinalis* have been widely used in treating thrombotic stroke, gastrointestinal complaints, anxiety and nervous stroke, etc. Honokiol, an active component purified from *M. officinalis*, has been demonstrated to have anti-inflammatory effects *in vitro* and *in vivo* [1,2]. Honokiol also has antibacterial and anxiolytic effects [3–5]. Previous studies revealed that honokiol had anti-tumor effects on RKO human colon cancer cells [6], CH27 human squamous lung cancer cells [7] and HL-60 human leukemia cells [8], in which apoptosis was involved. Evidence shows that honokiol could alter Ca^{2+} homeostasis in several cell types. Honokiol was shown to increase intracellular Ca^{2+} concentration ($[Ca^{2+}]_i$) leading to death of neonatal rat cortical neurons and SH-SY5Y human neuroblastoma cells [9]. However, the relationship between apoptosis and a Ca^{2+} signal in human glioblastoma cells is unclear.

* Corresponding author. Tel.: +886 7 3422121x1509; fax: +886 7 3468056.
E-mail address: pseudoo67@gmail.com (C.-R. Jan).

http://dx.doi.org/10.1016/j.cbi.2014.07.012
0009-2797/

Ca^{2+} is a highly versatile intracellular signal, controlling numerous cellular processes, such as cell proliferation, development, division, migration, contraction, fertilization, gene expression, secretion and death [10]. It has been reported that Ca^{2+}-related cell death could be triggered by large, sustained increases in $[Ca^{2+}]_i$ [11]. Although evidence shows that abnormal $[Ca^{2+}]_i$ levels can promote cell death through apoptosis [12], Ca^{2+}-independent apoptosis could also be found in different cell types such as human ovarian carcinoma cells [13]. Therefore the role of a $[Ca^{2+}]_i$ rise in apoptosis needs to be established for each stimulant and cell type [14–15].

Apoptosis is a physiological cell death process that is involved in the selective elimination of mutated, infected or dispensable cells; but failure of apoptosis can result in cancer and diseases [16–17]. In mammals, many of the signals that elicit apoptosis converge into mitochondria, which respond to proapoptotic signals [18–19]. Mitochondria play a key role in the apoptotic process, which involves permeabilization of the outer mitochondrial membrane and activation of a series of events that lead to cell death. The contribution of mitochondria to apoptosis was described in terms of disruption of the mitochondrial membrane potential, which resulted in the release of cytochrome c and activation of caspase [20].

It has been shown that honokiol induced apoptosis in different cancer cells, such as RKO human colorectal cancer cells [21] and SU-DHL4 human multiple myeloma cells [22]. Although honokiol had various effects on different models, the effect of honokiol on apoptosis in human glia cells is unclear. Glioblastoma multiforme (GBM) is the most common type of primary brain tumor in adults. Manipulated induction of apoptosis has the potential of treatment of GBM [23]. DBTRG-05MG human glioblastoma cells were chosen in this study. This cell is a well-differentiated, transformed tumorigenic line, and is a suitable model for research on cultured glial-type cells [24].

This study was aimed to explore the mechanisms underlying the effects of honokiol on $[Ca^{2+}]_i$, cell viability and apoptosis in DRTBG-05MG human glioblastoma cells. Fura-2 was used as a Ca^{2+}-sensitive dye to measure $[Ca^{2+}]_i$. The $[Ca^{2+}]_i$ rises were characterized, the concentration–response plots were established, and the pathways underlying the Ca^{2+} entry and Ca^{2+} release were explored. The cytotoxic effect of honokiol and the involvement of apoptotic pathway were investigated.

2. Materials and methods

2.1. Chemicals

The reagents for cell culture were from Gibco® (Gaithersburg, MD, USA). Fura-2-AM and BAPTA-AM were from Molecular Probes® (Eugene, OR, USA). Honokiol and all other reagents were from Sigma–Aldrich (St. Louis, MO, USA).

2.2. Cell culture

DBTRG-05MG human glioblastoma cells purchased from Bioresource Collection and Research Center (Taiwan) were cultured in RPMI-1640 medium supplemented with 10% heat-inactivated fetal bovine serum, 100 U/mL penicillin and 100 μg/mL streptomycin at 37 °C in a humidified 5% CO_2 atmosphere.

2.3. Experimental solutions

Ca^{2+}-containing medium (pH 7.4) contained 140 mM NaCl, 5 mM KCl, 1 mM $MgCl_2$, 2 mM $CaCl_2$, 10 mM HEPES, and 5 mM glucose. Ca^{2+}-free medium (pH 7.4) contained 140 mM NaCl, 5 mM KCl, 3 mM $MgCl_2$, 0.3 mM EGTA, 10 mM HEPES, and 5 mM glucose. Lysis buffer (pH 7.5) contained 20 mM Tris, 150 mM NaCl, 1 mM EDTA, 1 mM EGTA, 1% Triton, 2.5 mM sodium pyrophosphate, 1 mM β-glycerophosphate, 1 mM Na_3VO_4, 1 μg/mL leupeptin and 1 mM phenylmethylsulfonyl fluoride. TBST (pH 7.5) contained 25 mM Tris, 150 mM NaCl and 0.1% (v/v) Tween 20. Phosphate buffer saline (PBS, pH 7.4) contained 137 mM NaCl, 10 mM phosphate, 2.7 mM KCl. Reagents are dissolved in water, ethanol or dimethyl sulfoxide (DMSO) as concentrated stocks. Honokiol was dissolved in DMSO as a 0.1 M stock solution. The other reagents were dissolved in water, ethanol or DMSO. The concentration of organic solvents in the experimental solution was less than 0.1%, and did not alter basal $[Ca^{2+}]_i$, cell viability, apoptosis, mitochondrial membrane potential or reactive oxygen species (ROS) levels.

2.4. $[Ca^{2+}]_i$ measurements

Confluent cells grown on 6 cm dishes were trypsinized and made into a suspension in RPMI-1640 medium at a density of 1×10^6 cells/mL. Cell viability (>95%) was assured by trypan blue exclusion. The viability was routinely greater than 95% after the treatment. Cells were loaded with 2 μM fura-2-AM for 30 min at 25 °C in the same medium. Cells were subsequently washed with Ca^{2+}-containing medium twice and was made into a suspension in Ca^{2+}-containing medium at a density of 1×10^7 cells/mL. Fura-2 fluorescence measurements were performed in a water-jacketed cuvette (25 °C) with continuous stirring; the cuvette had 1 mL of medium and 0.5 million cells. Fluorescence was recorded with a Shimadzu RF-5301PC spectrofluorophotometer immediately after 0.1 mL cell suspension was added to 0.9 mL Ca^{2+}-containing or Ca^{2+}-free medium, by measuring excitation signals at 340 nm and 380 nm and emission signal at 510 nm at 1-s intervals. During the recording, reagents were added to the cuvette by pausing the recording for 3 s to open and close the cuvette-containing chamber. For calibration of $[Ca^{2+}]_i$, after completion of the experiments, the detergent Triton X-100 (0.1%) and $CaCl_2$ (5 mM) were added to the cuvette to obtain the maximal fura-2 fluorescence. The Ca^{2+} chelator EGTA (10 mM) was subsequently added to the cuvette to chelate Ca^{2+} and obtain the minimal fura-2 fluorescence. Control experiments showed that cells bathed in a cuvette with 80 μM honokiol had a viability of 95% after 20 min of fluorescence measurements. $[Ca^{2+}]_i$ was calculated as described previously [25].

Mn^{2+} quenching of fura-2 fluorescence was performed in Ca^{2+}-containing medium containing 50 μM $MnCl_2$. $MnCl_2$ was added to cell suspension in the cuvette 1 min before starting the fluorescence recording. Data were recorded at excitation signal at 360 nm (Ca^{2+}-insensitive) and emission signal at 510 nm at 1-s intervals as described previously [26].

2.5. Cell viability assays

The measurement of cell viability was based on the ability of cells to cleave tetrazolium salts by dehydrogenases. The intensity of developed color directly correlated with the number of live cells. Assays were performed according to manufacturer's instructions specifically designed for this assay (Roche Molecular Biochemical, Indianapolis, IN, USA). Cells were seeded in 96-well plates at a density of 10,000 cells/well in culture medium for 24 h in the presence of honokiol. The cell viability detecting reagent 4-[3-[4-lodophenyl]-2-4(4-nitrophenyl)-2H-5-tetrazolio-1,3-benzene disulfonate] (WST-1; 10 μL pure solution) was added to samples after treatment with honokiol, and cells were incubated for 30 min in a humidified atmosphere. In experiments using BAPTA-AM to chelate cytosolic Ca^{2+}, cells were treated with 5 μM BAPTA-AM for 1 h prior to incubation with honokiol. The cells were washed once with Ca^{2+}-containing medium and incubated with/without honok-

iol for 24 h. The absorbance of samples (A450) was determined using a multiwall plate reader. Absolute optical density was normalized to the absorbance of unstimulated cells in each plate and expressed as a percentage of the control value.

2.6. Alexa® Fluor 488 annexin V/propidium iodide (PI) staining for apoptosis

Annexin V/PI staining assay was employed to further detect cells in early apoptotic and late apoptotic/necrotic stages. Cells were exposed to honokiol at concentrations of 20–60 μM for 24 h. Cells were harvested after incubation and washed in cold phosphate-buffered saline (PBS). Cells were resuspended in 400 μL solution with 10 mM of HEPES, 140 mM of NaC1, 2.5 mM of $CaC1_2$ (pH 7.4). Alexa Fluor 488 annexin V/PI staining solution (Probes Invitrogen, Eugene, OR, USA) was added in the dark. After incubation for 15 min, the cells were collected and analyzed in a FACScan flow cytometry analyzer. Excitation wavelength was at 488 nm and the emitted green fluorescence of annexin V (FL1) and red fluorescence of PI (FL2) were collected using 530 nm and 575 nm bands pass filters, respectively. A total of at least 20,000 cells were analyzed per sample. Light scatter was measured on a linear scale of 1024 channels and fluorescence intensity was on a logarithmic scale. The amount of early apoptosis and late apoptosis/necrosis were determined, respectively, as the percentage of annexin V^+/PI^- or annexin V^+/PI^+ cells. Data were later analyzed using the flow cytometry analysis software WinMDI 2.8 (by Joe Trotter, freely distributed software). The *x* and *y* coordinates refer to the intensity of fluorescence of annexin V and PI, respectively.

2.7. Measurements of intracellular contents of ROS

Cells cultured on 6-well plates were treated with 20–60 μM honokiol for 24 h. Subsequently, cells were trypsinized and made into suspensions (1×10^6 cells/mL). For measuring intracellular H_2O_2 or O_2^- content, cells were treated with the general indicator probe dichlorofluorescein diacetate (DCFH-DA) or hydroethidine (HE) that responds to changes in intracellular redox status. Cells were incubated with 10 μM membrane-permeable probe DCFH-DA or 160 μM HE for 30 min at 37 °C. Inside cells, the acetate moieties of DCFH-DA were cleaved and oxidized, primarily by H_2O_2, to green fluorescent 2′-7-′-dichlorofluorescein (DCF). HE was oxidized primarily by O_2^- to form ethidium brom-ide (EB), which emitted red fluorescence [27]. Flow cytometry was performed by using a flowcytometer (FACScan; Becton Dickinson, Mountain View, CA, USA). A 15-mm air-cooled argon-ion laser was used to excite fluorescent DCF at 488 nm, and the emitted fluorescence was measured using a 530/30 nm band-pass optical filter. Ethidium fluorescence was excited at 488 nm and collected using a 585/21 nm band-pass optical filter. Samples were run using 10,000 cells per test sample. Data were analyzed using the CELL QUEST programs (CELLQUESTWIRELESS, Flushing, MI, USA).

2.8. Measurement of mitochondrial membrane potential

To measure the mitochondrial membrane potential, the MitoProbe™ 1,1′,3,3,3′,3′-hexamethylindodicarbocyanine iodide ($DiIC_1$) (5) assay kit (Molecular Probes® (Eugene, OR, USA)) was used as instructed by the manufacturer. Briefly, cells cultured on 6-well plates were treated with 20–60 μM honokiol for 24 h. Cells (including floating cells) grown in 6-well plates were collected following mild trypsinization. Trypsinized cells were washed once with PBS, and the cells were resuspended in 500 μL of PBS. Resuspended cells were labeled with 50 nM $DiIC_1$ (5) (excitation/emission, 638/658 nm) at 37 °C in the dark for 30 min. Labeled cells were washed once in PBS, and they were analyzed by fluorescence-activated cell sorting using a CyAn (DakoCytomation) high performance flow cytometer.

2.9. Assessment of cytosolic cytochrome c and cleavage caspase-9/caspase-3 level by Western immunoblotting

Cell concentrations were adjusted to 3×10^6 cells/dish and seeded to 6 cm culture dishes. After 2 h of incubation, the culture medium was replaced by serum-free medium supplemented with 1 mg/ml bovine serum albumin (USB™, Cleveland, OH, USA) and serum starvation was continued for 4 h, followed by addition of 20–60 μM honokiol for 24 h. The treatments were terminated by aspirating the supernatant and then washing the dishes with PBS. The cells were lysed on ice for 5 min with 70 μL of lysis buffer. The cell lysates were centrifuged to remove insoluble materials; and the protein concentration of each sample was measured. Approximately 50 μg of supernatant protein from each sample was used for gel electrophoresis analysis on a 10% SDS–polyacrylamide gel. The fractionated proteins on gel were transferred to PVDF membranes (NEN™ Life Science Products, Inc., Boston, MA, USA). For immuoblotting, the membranes were blocked with 5% non-fat milk in TBST and incubated overnight with the primary antibody (rabbit anti-human cytosolic cytochrome c, rabbit anti-human cleavage caspase-9/caspase-3 or rabbit anti-human β-actin; all from Cell Signaling Technology, Beverly, MA, USA). Then the membranes were extensively washed with TBST and incubated for 60 min with the secondary antibody (goat anti-rabbit antibody or goat anti-mouse antibody, Transduction Laboratories, Lexington, KY, USA). After extensive washing with TBST, the immune complexes were detected by chemiluminescence using the Renaissance™ Western Blot Chemiluminescence Reagent Plus kit (NEN™).

2.10. Statistics

Data are reported as mean ± S.E.M. of three separate experiments. Data were analyzed by one-way analysis of variances (ANOVA) using the Statistical Analysis System (SAS®, SAS Institute Inc., Cary, NC, USA). Multiple comparisons between group means were performed by post hoc analysis using the Tukey's HSD (honestly significantly difference) procedure. A *P*-value less than 0.05 were considered significant.

3. Results

3.1. Honokiol concentration-dependently induced a $[Ca^{2+}]_i$ rise in Ca^{2+}-containing medium or Ca^{2+}-free medium

The effect of honokiol on basal $[Ca^{2+}]_i$ was examined. Fig. 1A shows that the basal $[Ca^{2+}]_i$ was 50 ± 2 nM. At concentrations between 20 μM and 80 μM, honokiol induced a $[Ca^{2+}]_i$ rise in a concentration-dependent manner in Ca^{2+}-containing medium. At a concentration of 10 μM, honokiol did not alter $[Ca^{2+}]_i$. At a concentration of 80 μM, honokiol induced a $[Ca^{2+}]_i$ rise that attained to a net (baseline subtracted) increase of 298 ± 3 nM ($n = 3$) followed by a decay. The Ca^{2+} response saturated at 80 μM honokiol because 100 μM honokiol evoked a similar response as that induced by 80 μM honokiol. Fig. 1B shows that in Ca^{2+}-free medium, 80 μM honokiol induced a $[Ca^{2+}]_i$ rise of 155 ± 3 nM; and at a concentration of 20 μM, honokiol induced a $[Ca^{2+}]_i$ rise of 58 ± 3 nM. Fig. 1C shows the concentration–response plots of honokiol-induced responses. The EC_{50} value was 38 ± 3 μM or 58 ± 3 μM in Ca^{2+}-containing medium or Ca^{2+}-free medium, respectively, fitting to a Hill equation. Honokiol between 20 μM

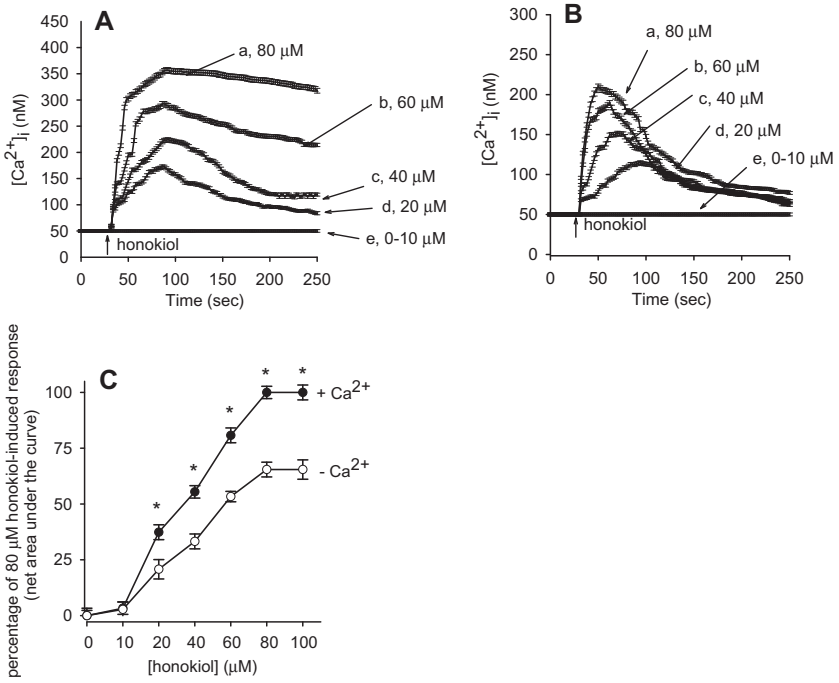

Fig. 1. Honokiol-induced $[Ca^{2+}]_i$ rises in fura-2-loaded human glioblastoma cells. (A) Honokiol was added to cells at 25 s at concentrations indicated. Ca^{2+}-containing medium was used in these experiments. (B) Honokiol-induced $[Ca^{2+}]_i$ rises in Ca^{2+}-free medium. Honokiol was added at 25 s. (C) Plots of concentration–response relationship of honokiol-evoked $[Ca^{2+}]_i$ rises in the presence or absence of extracellular Ca^{2+}. The *y* axis is the percentage of the net (baseline subtracted) area under the curve (25–250 s) of the $[Ca^{2+}]_i$ rise induced by 80 μM honokiol in Ca^{2+}-containing medium. Data are mean ± S.E.M. of three separate experiments. $^*P < 0.05$ compared to open circles. Data are mean ± S.E.M. of three separate experiments.

and 100 μM did not induce a $[Ca^{2+}]_i$ rise in other cell types including MDCK canine renal tubular cells, OC2 human oral cancer cells, PC3 human prostate cancer cells and MG63 human osteosarcoma cells (data not shown).

3.2. Honokiol-induced $[Ca^{2+}]_i$ rise involved Ca^{2+} influx as assayed by measuring Mn^{2+} influx

Experiments were performed to confirm that honokiol-induced $[Ca^{2+}]_i$ rise involved Ca^{2+} influx. Because Mn^{2+} enters cells through similar pathways as Ca^{2+} but quenches fura-2 fluorescence at all excitation wavelengths [26], quenching of fura-2 fluorescence excited at the Ca^{2+}-insensitive excitation wavelength of 360 nm by Mn^{2+} implies Ca^{2+} influx. Fig. 2 shows that 80 μM honokiol induced an immediate decrease in the 360 nm excitation signal by 35 ± 3 ($n = 3$) arbitrary units (trace b compared to trace a). This suggests that honokiol-induced $[Ca^{2+}]_i$ rise involved Ca^{2+} influx.

3.3. Store-operated Ca^{2+} channel blockers did not affect honokiol-induced $[Ca^{2+}]_i$ rise, but PKC inhibitor decreased honokiol-induced $[Ca^{2+}]_i$ rise

Fig. 1 shows that honokiol-induced Ca^{2+} response saturated at 80 μM; thus in the following experiments the response induced by 80 μM honokiol was used as control. The store-operated Ca^{2+} channel blockers nifedipine (1 μM), econazole (0.5 μM) and SK&F96365 (5 μM); the PKC activator phorbol 12-myristate 13 acetate (PMA; 1 nM) and the PKC inhibitor GF109203X (2 μM) were applied 1 min before 80 μM honokiol in Ca^{2+}-containing medium. Addition of nifedipine, econazole, SK&F96365, PMA, or GF109203X alone did not alter baseline $[Ca^{2+}]_i$ (data not shown). In Ca^{2+}-containing medium, only GF109203X inhibited honokiol-induced $[Ca^{2+}]_i$ rise by 54 ± 2% ($P < 0.05$; Fig. 3A). Fig. 3B shows that

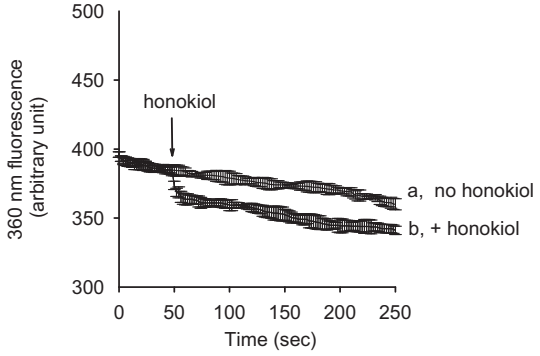

Fig. 2. Effect of honokiol on Ca^{2+} influx by measuring Mn^{2+} quenching of fura-2 fluorescence. Experiments were performed in Ca^{2+}-containing medium. $MnCl_2$ (50 μM) was added to cells 1 min before fluorescence measurements. The *y* axis is fluorescence intensity (in arbitrary units) measured at the Ca^{2+}-insensitive excitation wavelength of 360 nm and the emission wavelength of 510 nm. Honokiol (80 μM) was added as indicated. Data are mean ± S.E.M. of three separate experiments.

in Ca^{2+}-free medium, GF109203X also inhibited honokiol-induced $[Ca^{2+}]_i$ rise by 62 ± 2% ($P < 0.05$).

3.4. Endoplasmic reticulum was the dominant Ca^{2+} store in honokiol-induced Ca^{2+} release

Because the endoplasmic reticulum is the major Ca^{2+} store in most cells [28], efforts were made to explore the Ca^{2+} store involved in honokiol-induced Ca^{2+} release. Fig. 4A shows that in Ca^{2+}-free medium, addition of 80 μM honokiol prevented the $[Ca^{2+}]_i$ rise induced by thapsigargin (TG; 1 μM), an inhibitor of endoplasmic reticulum Ca^{2+} pumps [29]. Fig. 4B shows that TG

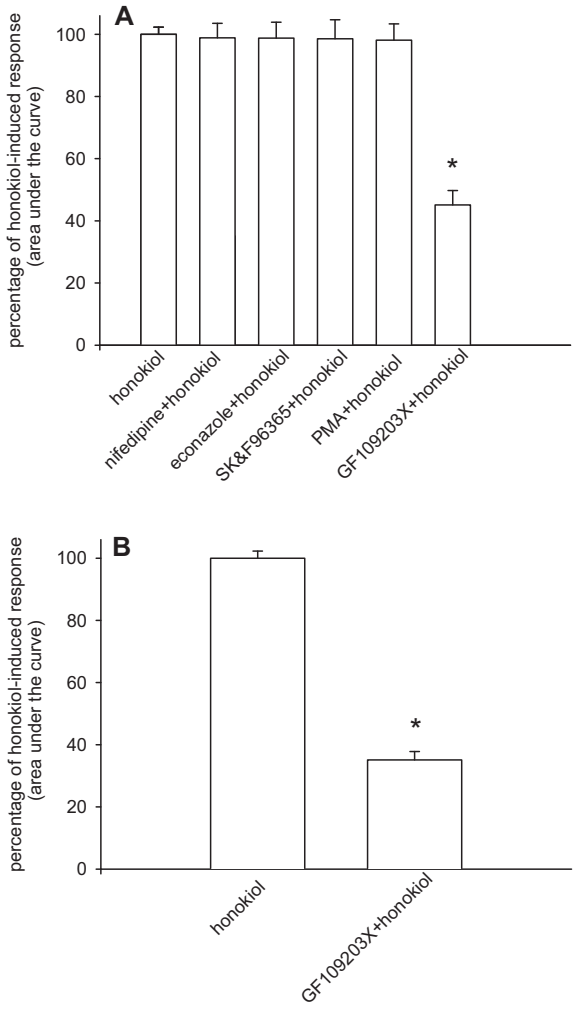

Fig. 3. Effect of Ca^{2+} channel modulators on honokiol-induced $[Ca^{2+}]_i$ rise. (A) The experiments were performed in Ca^{2+}-containing medium. In blocker- or modulator-treated groups, the reagent was added 1 min before honokiol (80 μM). The concentration was 1 μM for nifedipine, 0.5 μM for econazole, 5 μM for SK&F96365, 10 nM for phorbol 12-myristate 13-acetate (PMA), and 2 μM for GF109203X. Data are expressed as the percentage of 80 μM honokiol-induced $[Ca^{2+}]_i$ rise (150 s interval; net area under the curve), and are mean ± S.E.M. of three separate experiments. (B) Similar to (A), in Ca^{2+}-free medium, GF109203X (2 μM) was added 1 min before honokiol (80 μM). Data are mean ± S.E.M. of three separate experiments. $^*P < 0.05$ compared to 1st column.

induced a $[Ca^{2+}]_i$ rise of 125 ± 3 nM, and subsequently added 80 μM honokiol failed to induce a $[Ca^{2+}]_i$ rise. Another endoplasmic reticulum Ca^{2+} pump inhibitor 2,5-di-tert-butylhydroquinone (BHQ; 50 μM) [30] was used to confirm the TG's effect. Fig. 4C shows that BHQ did not induce a $[Ca^{2+}]_i$ rise after honokiol incubation. Conversely, Fig. 4D shows that BHQ evoked a $[Ca^{2+}]_i$ rise of 99 ± 3 nM, and subsequently added honokiol had no effect on $[Ca^{2+}]_i$.

3.5. Honokiol induced $[Ca^{2+}]_i$ rises in a phospholipase C (PLC)-dependent pathway

PLC-dependent production of inositol 1,4,5-trisphosphate (IP_3) plays an important role in releasing Ca^{2+} from the endoplasmic reticulum [31]. Because honokiol released Ca^{2+} from the endoplasmic reticulum, the role of PLC in this process was examined. U73122, a PLC inhibitor in glial cell line [32], was used to see whether the activation of this enzyme was required for honokiol-induced Ca^{2+} release. First, effort was exerted to assure the effectiveness of U73122 as a PLC inhibitor under our experimental condition. ATP is a well-known PLC-dependent agonist of $[Ca^{2+}]_i$ rise in most cell types including glia cells [33]. Fig. 5 shows that incubation with 2 μM U73122 did not change basal $[Ca^{2+}]_i$ but abolished ATP-induced $[Ca^{2+}]_i$ rise. This suggests that U73122 effectively suppressed PLC activity. Fig. 5 shows that 80 μM honokiol-evoked $[Ca^{2+}]_i$ rises were set as 100% (control). Incubation with U73122 inhibited honokiol-induced $[Ca^{2+}]_i$ rises and the combination of U73122 and ATP also inhibited honokiol-induced $[Ca^{2+}]_i$ rises.

3.6. Honokiol decreased cell viability that was not triggered by a preceding $[Ca^{2+}]_i$ rise

Because abnormal $[Ca^{2+}]_i$ rises may cause cell death, experiments were performed to examine whether honokiol-induced cytotoxicity was triggered by a preceding $[Ca^{2+}]_i$ rise in DBTRG-05MG cells. The intracellular Ca^{2+} chelator BAPTA-AM [34] was used to prevent a $[Ca^{2+}]_i$ rise during honokiol treatment. Fig. 6A shows that 5 μM BAPTA-AM loading abolished 80 μM honokiol-induced $[Ca^{2+}]_i$ rise in Ca^{2+}-containing medium. This suggests that BAPTA-AM effectively prevented a rise in $[Ca^{2+}]_i$ during honokiol treatment. In Fig. 6B, cells were treated with 0–80 μM honokiol for 24 h. In the presence of 20–80 μM honokiol, cell viability decreased in a concentration-dependent manner. Fig. 6B also shows that 5 μM BAPTA-AM loading did not change the control value of cell viability. In the presence of 20–80 μM honokiol, BAPTA-AM loading did not affect honokiol-induced cell death. This suggests that honokiol induced cell death that was not triggered by a preceding $[Ca^{2+}]_i$ rise.

3.7. Honokiol induced cell death involved apoptosis

Because apoptosis plays an important role in cell death, the next set of experiments explored whether honokiol-induced cell death involved apoptosis. Annexin V/PI staining was applied to detect apoptotic cells after honokiol treatment. Fig. 7A and B shows that treatment with 20–60 μM honokiol significantly induced apoptosis in DBTRG-05MG cells in a concentration-dependent manner.

3.8. Honokiol induced apoptosis involved ROS production

Since ROS was thought to be involved in honokiol-induced apoptosis in human hepatoma cells [35], efforts were made to explore the effect of honokiol on H_2O_2 or O_2^- production in human glioblastoma cells. The results show that DCF fluorescence (Fig. 8A and C) or EB fluorescence intensity (Fig. 8B and D) was increased in honokiol-treated cells, respectively.

3.9. A role of mitochondria-dependent apoptotic cascade in honokiol-induced cell death

Since mitochondrial membrane potential is related to the apoptotic pathway [19], experiments were performed to examine the mechanism underlying the death by measuring the change of mitochondrial membrane potential. Fig. 9A shows that ($DiIC_1$) (5) fluorescence intensity was decreased by treatment with 20–60 μM honokiol for 24 h in a concentration-dependent manner. Fig. 9B further shows that the depolarized cells were also increased in honokiol-treated cells. Because the release of cytochrome c from mitochondria and the cleavage of caspases-9/caspase-3 are associated with the mitochondrial pathway of apoptosis [17,19], experiments were conducted to explore whether honokiol released cytochrome c and activated caspase-9/caspase-3. Fig. 9C and D

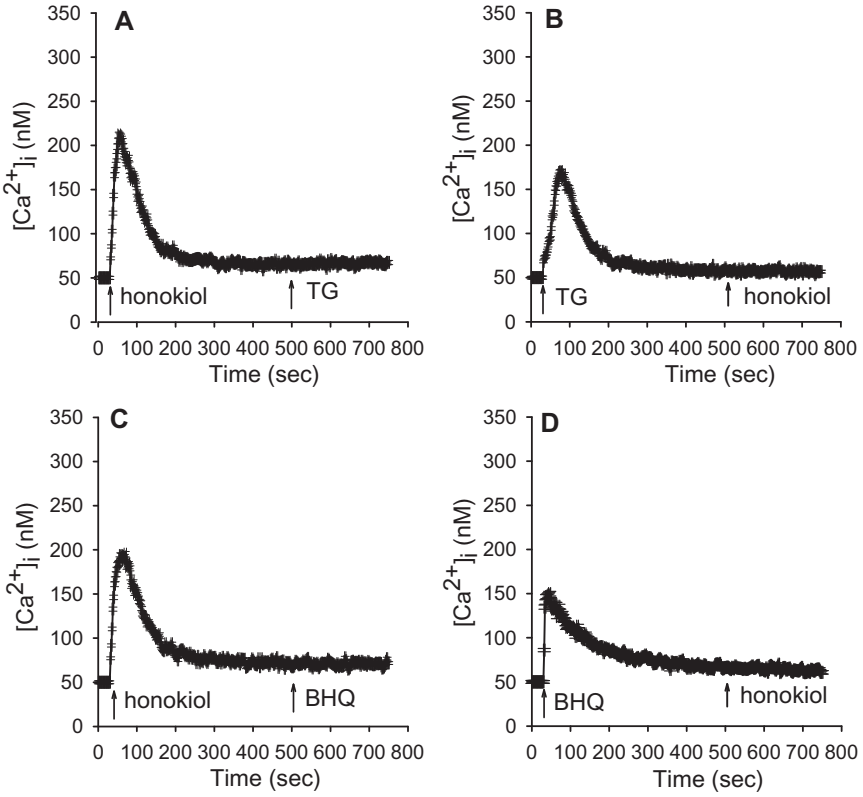

Fig. 4. Ca^{2+} stores for honokiol-induced Ca^{2+} release. (A–D) Experiments were performed in Ca^{2+}-free medium. Honokiol (80 μM), thapsigargin (TG; 1 μM) and BHQ (50 μM) were added at time points indicated. Data are mean ± S.E.M. of three separate experiments.

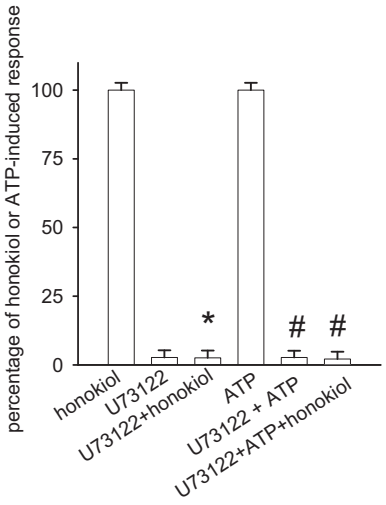

Fig. 5. U73122-induced inhibition of honokiol-induced Ca^{2+} release. Experiments were performed in Ca^{2+}-free medium. First column is the 80 μM honokiol-induced $[Ca^{2+}]_i$ rise. Second column shows that 2 μM U73122 did not alter basal $[Ca^{2+}]_i$. Third column shows that U73122 pretreatment for 200 s abolished 80 μM honokiol-induced $[Ca^{2+}]_i$ rise ($^*P < 0.05$ compared to 1st column). Fourth column shows the ATP-induced $[Ca^{2+}]_i$ rise compared to honokiol control. Fifth column shows that U73122 pretreatment for 200 s abolished ATP-induced $[Ca^{2+}]_i$ rise ($^{\#}P < 0.05$ compared to 4th column). Sixth column shows that U73122 and ATP pretreatment (for 200 s and 50 s, respectively) abolished 80 μM honokiol-induced $[Ca^{2+}]_i$ rise ($^{\#}P < 0.05$ compared to 4th column). Data are mean ± S.E.M. of three separate experiments.

show that cytosolic cytochrome c level was increased by treatment with 20–60 μM honokiol for 24 h. Fig. 9E and F show that cleaved caspase-9 level was increased by treatment with 20–60 μM honokiol for 24 h. Figs. 9G and H show that cleaved caspase-3 level was increased by treatment with 20–60 μM honokiol for 24 h.

4. Discussion

Ca^{2+} homeostasis plays a key role in the function of almost all cell types including human glioblastoma cells. In this cell, a rise in $[Ca^{2+}]_i$ affects cell migration, invasion or viability [36]. A previous study showed that prolactin and thapsigargin increased $[Ca^{2+}]_i$ and transmitted cell homeostasis signaling pathway in human glioblastoma cells [37–38]. Honokiol was shown to induce apoptosis in human glioblastoma cells [39], but the relationship between honokiol-induced apoptosis and Ca^{2+} signaling in this cell is unclear. In our study, the results show that honokiol induced a concentration-dependent $[Ca^{2+}]_i$ rise in DBTRG-05MG human glioblastoma cells. Interestingly, honokiol did not have similar effects on four other types of cells including MDCK canine renal tubular cells, OC2 human oral cancer cells, PC3 human prostate cancer cells and MG63 human osteosarcoma cells. This is consistent with previous studies that honokiol induced a $[Ca^{2+}]_i$ rise in two different lines of neuronal cells including rat cortical neurons and SH-SY5Y human neuroblastoma cells [9]. Therefore, the combined evidence suggests that the stimulatory effect of honokiol on $[Ca^{2+}]_i$ is most likely restricted to neuronal cells.

Honokiol elevated $[Ca^{2+}]_i$ by depleting intracellular Ca^{2+} stores and inducing Ca^{2+} entry from extracellular medium because removing extracellular Ca^{2+} reduced a part of honokiol-induced $[Ca^{2+}]_i$ rise. Mn^{2+} quenching data also suggest that honokiol induced Ca^{2+} entry. The magnitude of honokiol-induced Mn^{2+} quenching did not change during the measurement of 200 s, sug-

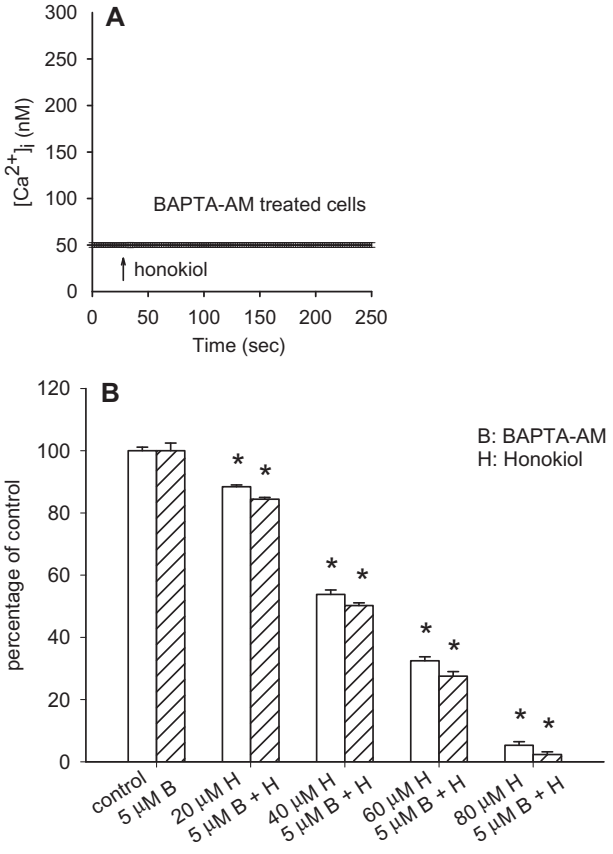

Fig. 6. Effect of honokiol on cell viability. (A) Following BAPTA-AM treatment, cells were incubated with fura-2-AM as described in Methods. Then $[Ca^{2+}]_i$ measurements were conducted in Ca^{2+}-containing medium. Honokiol (80 μM) was added as indicated. (B) Cells were treated with 0–80 μM honokiol for 24 h, and cell viability assay was conducted. Data are mean ± S.E.M. of three separate experiments. Each treatment had six replicates (wells). Data are expressed as percentage of control that is the increase in cell numbers in honokiol-free groups. Control had 11,587 ± 656 cells/well before experiments, and 12,458 ± 715 cells/well after incubation for 24 h. $^{*}P < 0.05$ compared to control. In each group, the Ca^{2+} chelator BAPTA-AM (5 μM) was added to cells followed by treatment with honokiol in Ca^{2+}-containing medium. Cell viability assay was subsequently performed.

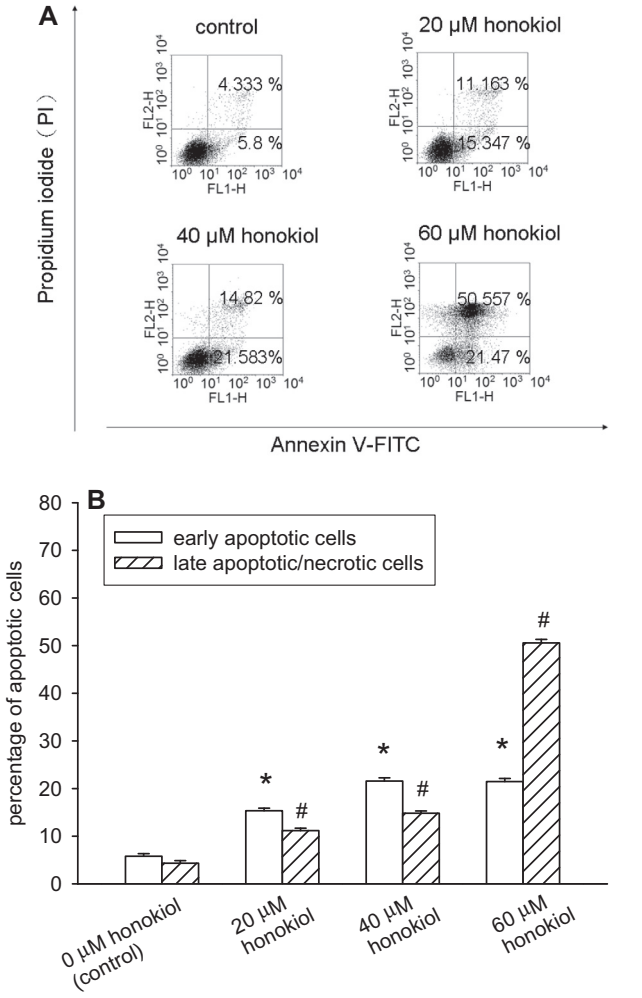

Fig. 7. Honokiol-induced cell death involved apoptosis. (A) Cells were treated with 0–60 μM honokiol for 24 h. Cells were then processed for annexin V/PI staining and analyzed by flow cytometry. (B) The percentage of early apoptotic cells and late apoptotic/necrotic cells. $^{*,\#}P < 0.05$ compared with control. Data are mean ± S.E.M. of three separate experiments.

gesting that Mn^{2+} influx continuously occurred throughout this interval.

Since glioblastoma multiforme (GBM) tumor cells have store-operated Ca^{2+} channels [40], a $[Ca^{2+}]_i$ rise in DBTRG-05MG human glioblastoma cells may also be induced by Ca^{2+} entry via this channels. Therefore, the mechanism of honokiol-induced $[Ca^{2+}]_i$ rise was explored. The results suggest that honokiol did not cause Ca^{2+} influx via stored-operated Ca^{2+} entry because honokiol-induced Ca^{2+} entry was not inhibited by three store-operated Ca^{2+} entry blockers nifedipine, econazole and SK&F96365. These compounds have been shown to inhibit store-operated Ca^{2+} channels in different models [41–44] including human glioblastoma cells [45]. Menthol or alkyl phenols like honokiol have been shown to activate transient receptor potential (TRP) ion channels and induce Ca^{2+} entry in DBTRG-05MG human glioblastoma cells [46–47]. Therefore it is possible that TRP ion channels may be associated with honokiol-induced $[Ca^{2+}]_i$ rise. In terms of the Ca^{2+} stores involved in honokiol-induced Ca^{2+} release, the results show that TG/BHQ pretreatment both abolished honokiol-induced $[Ca^{2+}]_i$ rise, and conversely, honokiol pretreatment also inhibited TG/BHQ-induced Ca^{2+} release. Therefore, the TG/BHQ-sensitive endoplasmic reticulum stores appear to be the dominant one for honokiol-induced Ca^{2+} release.

The role of PKC activity in honokiol-induced $[Ca^{2+}]_i$ rise was examined because PKC activity is tightly coupled to Ca^{2+} signaling [48]. Previous studies showed that modulation of PKC activity affected $[Ca^{2+}]_i$ in U87 human glioblastoma cells [49]. In this study, inhibition of PKC by GF109203X suppressed honokiol-induced $[Ca^{2+}]_i$ rise, but activation of PKC by PMA did not have an effect on $[Ca^{2+}]_i$. Furthermore, GF109203X-induced inhibition was not altered by removal of extracellular Ca^{2+}. This suggests that PKC activity in honokiol-induced $[Ca^{2+}]_i$ rise was related to Ca^{2+} entry, not Ca^{2+} release. Therefore, it appears that a normally maintained PKC activity was necessary for a full response of 80 μM honokiol-induced $[Ca^{2+}]_i$ rise. In addition, one of the Ca^{2+} releasing mechanisms that utilize the endoplasmic reticulum store is via the PLC-dependent IP_3 pathway. Because honokiol-induced Ca^{2+} release was abolished when PLC activity was inhibited by U73122, it seems that the PLC pathway plays a dominant role in honokiol-induced Ca^{2+} release.

Previous studies showed that honokiol caused cytotoxicity in different cancer cells, such as SKOV3 human ovarian tumor cells

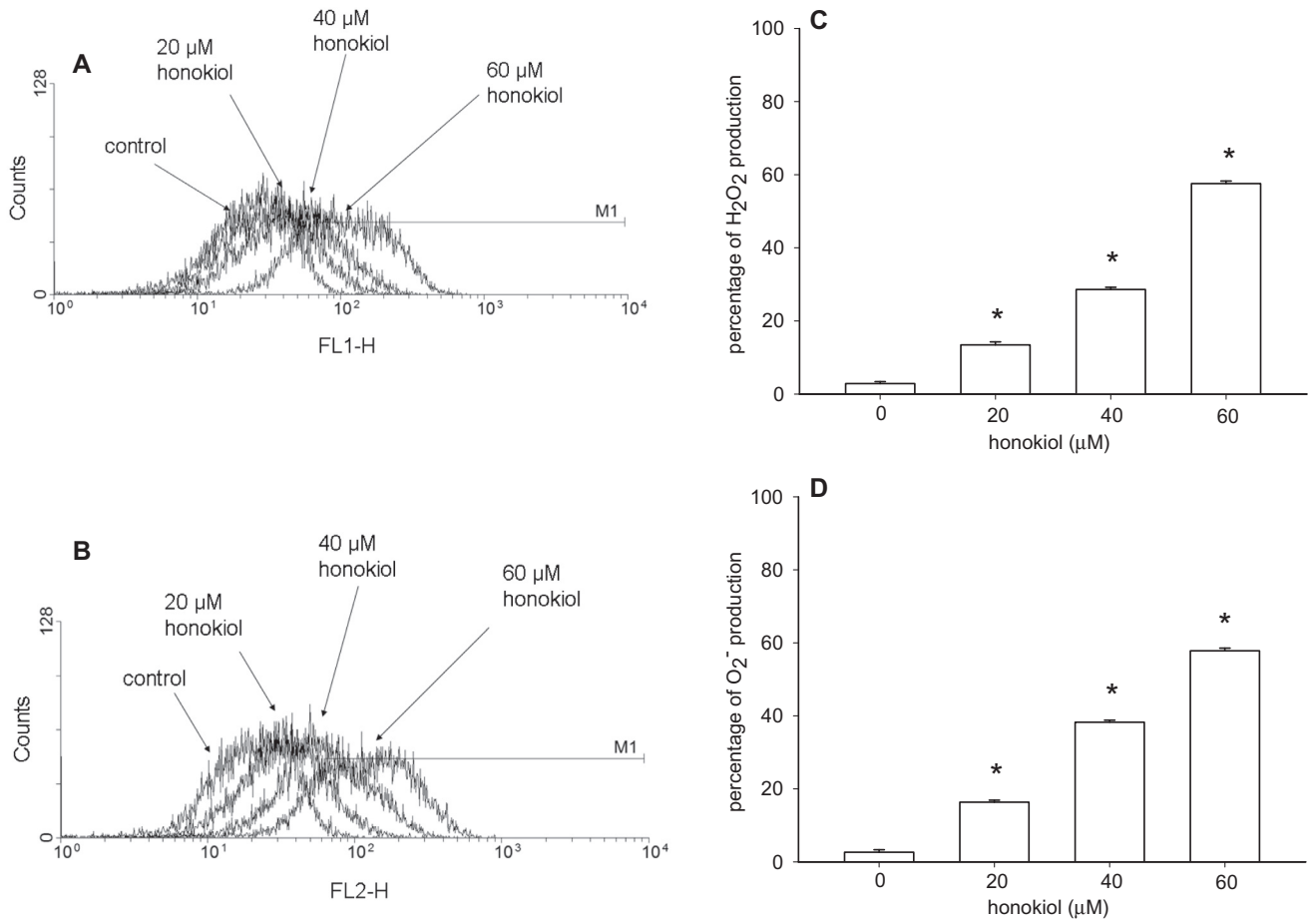

Fig. 8. Flow cytometric analysis of intracellular ROS content (H_2O_2 or O_2^-) in cells treated with honokiol. (A,B) A representative histogram showing changes between DCF and EB fluorescence intensity in untreated cells and cells treated with 20–60 μM honokiol for 24 h. (C,D) M1 represents the percentage of H_2O_2 or O_2^- production. A baseline level of H_2O_2 or O_2^- counts was obtained when cells were incubated only with phosphate buffered saline (PBS) and without 10 μM dichlorofluorescein diacetate (DCFH-DA) or 160 μM hydroethidine (HE) for 30 min at 37 °C. The baseline level of H_2O_2 was 0.05%. Honokiol (0, 20, 40 or 60 μM) increased the production of H_2O_2 by 2.9%, 13.5%, 28.6% or 57.6%, respectively (baseline level of H_2O_2 was subtracted). The baseline level of O_2^- was 0.05%. Honokiol (0, 20, 40 or 60 μM) increased the production of O_2^- by 2.6%, 16.3%, 38.3% or 57.8%, respectively (baseline level of O_2^- was subtracted). *$P < 0.05$ compared with control. Data are representative of three separate experiments.

[50]. Our data show that honokiol was cytotoxic to human glioblastoma cells in a concentration-dependent manner. Since honokiol induced both $[Ca^{2+}]_i$ rises and cell death, it would be interesting to know whether the death occurred in a Ca^{2+}-associated fashion. In this study, honokiol-induced cell death did not change when cytosolic Ca^{2+} was effectively chelated by BAPTA-AM. Thus it appears that honokiol-induced cell death was not triggered by a $[Ca^{2+}]_i$ rise. Although emptying of intracellular Ca^{2+} stores and/or influx of extracellular Ca^{2+} can modulate cell viability in different cell types [51], Ca^{2+}-dissociated cell death could be found in thymic lymphoma cells [52] and LNCaP human prostate cancer cells [53], etc.

It has been shown that many pro-apoptotic agents induce apoptosis via the mitochondrial pathway in different cancer cells [54]. In a previous study, honokiol increased ROS production, decreased the mitochondrial membrane potential leading to apoptosis in SMMC-7221 human hepatoma cells [35]. Therefore, this study examined whether mitochondrial pathway of apoptosis had a role in honokiol-induced apoptosis. The results show that honokiol at concentrations between 20 μM and 60 μM enhanced ROS production, decreased mitochondrial membrane potential, released cytochrome c and activated caspase-9/caspase-3. Thus honokiol appears to induce mitochondrial pathway of apoptosis in DBTRG-05MG human glioblastoma cells.

In vivo studies show that honokiol could effectively cross blood–brain barrier and blood–cerebrospinal fluid barrier [55] and inhibit brain tumor growth in rat intracerebral gliosarcoma model and human xenograft glioma model [56]. In this case, no BioResponse honokiol (BR-honokiol)-related adverse effects were reported at doses up to 20 mg. A single 20 mg dose of BR-honokiol resulted in a mean maximum brain concentration of 11.97 μg/mL (~46 μM) [56]. The concentrations used in our study were comparable to this *in vivo* report. Therefore, our data may have clinical relevance.

In sum, the oriental medicinal herb honokiol induced Ca^{2+} release from endoplasmic reticulum in a PLC-dependent manner and also caused Ca^{2+} entry through PKC-dependent, non-store-operated Ca^{2+} channels in human glioblastoma cells. So far, most of the studies performed to explore the relation between chemicals-induced $[Ca^{2+}]_i$ rises and apoptosis in several lines of human glioblastoma cells suggest that the apoptosis was triggered by a preceding $[Ca^{2+}]_i$ rise [40,57]. In contrast, our study shows that honokiol induced cell death that involved the mitochondrial pathway of apoptosis independent of a preceding $[Ca^{2+}]_i$ rise. Thus, it

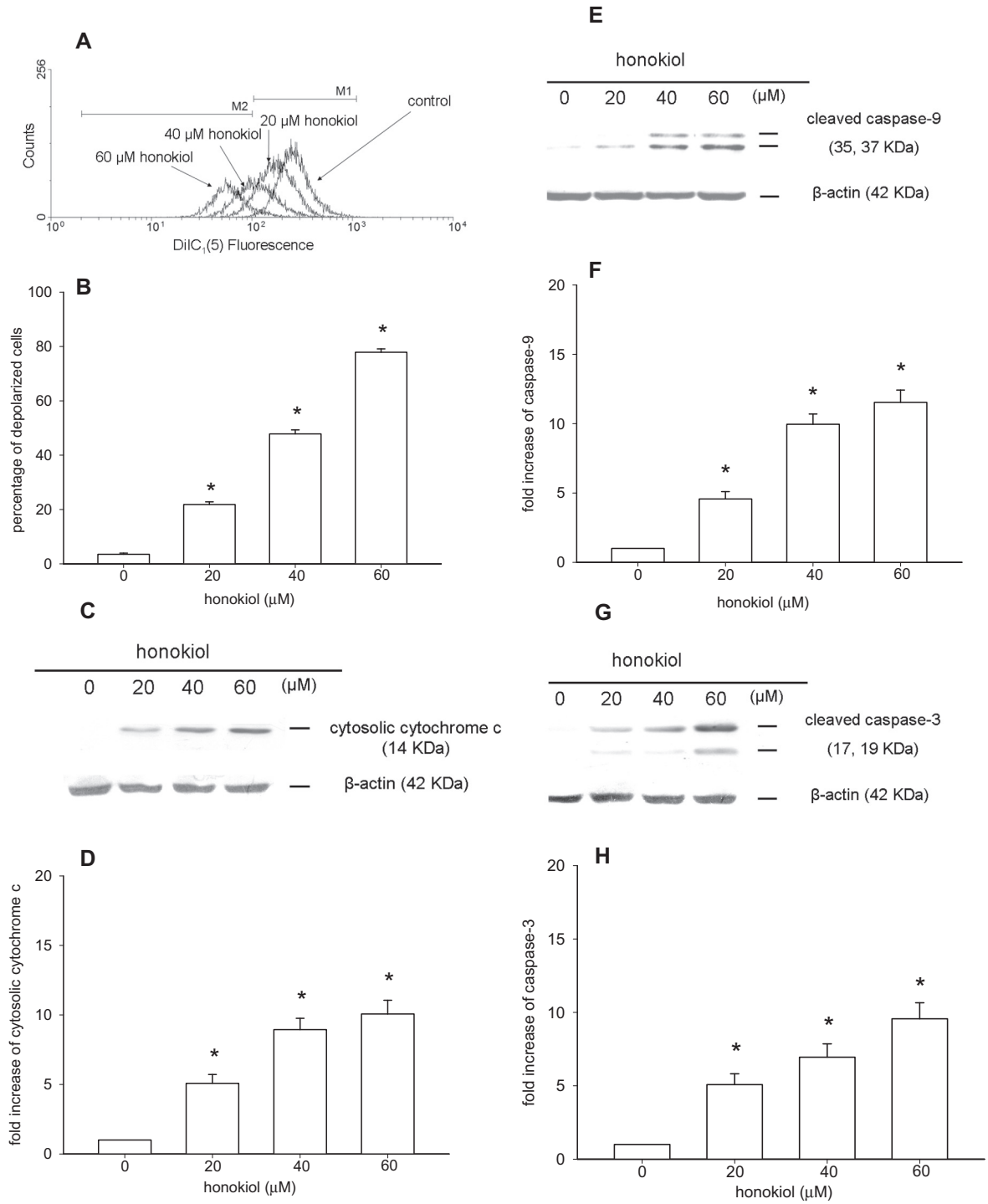

Fig. 9. Honokiol decreased mitochondrial membrane potential, released cytochrome c and activated caspase-9/caspase-3. (A) Cells were treated with various concentrations of honokiol for 24 h and then stained with $DiIC_1$ (5) and incubated at 37 °C for 30 min. The mean $DiIC_1$ (5) fluorescence intensity was detected using a flow cytometry. $DiIC_1$ (5) stain intensity decreases when cells are treated with reagents that disrupt mitochondrial membrane potential. M1 represents the percentage of total mitochondrial transmembrane potential cells. The baseline level of total mitochondrial transmembrane potential cells was obtained when cells were incubated only with 10 μM DiIC1 (5) for 30 min at 37 °C. The baseline level of total mitochondrial transmembrane potential cells was 100%. M2 represents the percentage of low-mitochondrial transmembrane potential cells. The baseline level of low-mitochondrial transmembrane potential cells was obtained when cells were incubated only with phosphate buffered saline (PBS) and without 10 μM DiIC1 (5) for 30 min at 37 °C. The baseline level of low-mitochondrial transmembrane potential cells was 0.05%. Honokiol (0, 20, 40 or 60 μM) increased the production of low-mitochondrial transmembrane potential cells by 2.6%, 22.3%, 45.7% or 78.2%, respectively (baseline level of low-mitochondrial transmembrane potential cells was subtracted). $^*P < 0.05$ compared with control. Data are representative of three separate experiments. (B) Data are expressed in percentage of cells displaying mitochondrial depolarization in honokiol-treated groups compared with controls. (C) Cytosolic cytochrome c level was increased in honokiol-induced apoptosis. Protein extracts were prepared 24 h after exposure to various concentrations of honokiol. Data are typical of three separate experiments. (D) The effect of honokiol on cytosolic cytochrome c level as quantified by densitometry. The figure normalized intensities of the bands of cytosolic cytochrome c against the bands of β-actin using NIH image 1.61. $^*P < 0.05$ compared with control. Data are representative of three separate experiments. (E, G) Caspase-9 or caspase-3 cysteine proteases were activated in honokiol-induced apoptosis. Protein extracts were prepared 24 h after exposure to various concentrations of honokiol. Data are typical of three separate experiments. (F, H) The effect of honokiol on activation of caspase-9 or caspase-3 is quantified by densitometry. The figure normalized intensities of the bands of cleaved caspase-3 against the bands of β-actin using NIH image 1.61. $^*P < 0.05$ compared with control. Data are representative of three separate experiments.

appears that, not only Ca^{2+}-associated, but also Ca^{2+}-dissociated apoptosis may occur in human glioblastoma cells, depending on the stimulant.

Conflict of Interest

The authors declare that there are no conflicts of interest.

Transparency Document

The Transparency document associated with this article can be found in the online version.

Acknowledgment

This work was supported by a grant from Kaohsiung Veterans General Hospital (VGHKS101-019) to C.-R. Jan.

References

[1] C.K. Chiang, M.L. Sheu, K.Y. Hung, K.D. Wu, S.H. Liu, Honokiol, a small molecular weight natural product, alleviates experimental mesangial proliferative glomerulonephritis, Kidney Int. 70 (2006) 682–689.
[2] J. Park, J. Lee, E. Jung, Y. Park, K. Kim, B. Park, K. Jung, E. Park, J. Kim, D. Park, *In vitro* antibacterial and anti-inflammatory effects of honokiol and magnolol against *Propionibacterium* sp., Eur. J. Pharmacol. 496 (2004) 189–195.
[3] A.M. Clark, F.S. El-Feraly, W.S. Li, Antimicrobial activity of phenolic constituents of *Magnolia grandiflora* L., J. Pharm. Sci. 70 (1981) 951–952.
[4] K. Watanabe, H. Watanabe, Y. Goto, M. Yamaguchi, N. Yamamoto, K. Hagino, Pharmacological properties of magnolol and honokiol extracted from *Magnolia officinalis*: central depressant effects, Planta Med. 49 (1983) 103–108.
[5] K.T. Liou, Y.C. Shen, C.F. Chen, C.M. Tsao, S.K. Tsai, Honokiol protects rat brain from focal cerebral ischemia–reperfusion injury by inhibiting neutrophil infiltration and reactive oxygen species production, Brain Res. 992 (2003) 159–166.
[6] T. Wang, F. Chen, Z. Chen, Y.F. Wu, X.L. Xu, S. Zheng, X. Hu, Honokiol induces apoptosis through p53-independent pathway in human colorectal cell line RKO, World J. Gastroenterol. 10 (2004) 2205–2208.
[7] S.E. Yang, M.T. Hsieh, T.H. Tsai, S.L. Hsu, Down-modulation of Bcl-X_L, release of cytochrome c and sequential activation of caspases during honokiol-induced apoptosis in human squamous lung cancer CH27 cells, Biochem. Pharmacol. 63 (2002) 1641–1651.
[8] W.F. Fong, A.K. Tse, K.H. Poon, C. Wang, Magnolol and honokiol enhance HL-60 human leukemia cell differentiation induced by 1,25-dihydroxyvitamin D_3 and retinoic acid, Int. J. Biochem. Cell Biol. 37 (2005) 427–441.
[9] H. Zhai, K. Nakade, Y. Mitsumoto, Y. Fukuyama, Honokiol and magnolol induce Ca^{2+} mobilization in rat cortical neurons and human neuroblastoma SH-SY5Y cells, Eur. J. Pharmacol. 474 (2003) 199–204.
[10] M.J. Berridge, M.D. Bootman, H.L. Roderick, Calcium signalling: dynamics, homeostasis and remodeling, Nat. Rev. Mol. Cell Biol. 4 (2003) 517–529.
[11] D.J. McConkey, S. Orrenius, The role of calcium in the regulation of apoptosis, Biochem. Biophys. Res. Commun. 239 (1997) 357–366.
[12] P. Nicotera, S. Orrenius, The role of calcium in apoptosis, Cell Calcium 23 (1998) 173–180.
[13] Y. Song, P. Wilkins, W. Hu, K.S. Murthy, J. Chen, Z. Lee, R. Oyesanya, J. Wu, S.E. Barbour, X. Fang, Inhibition of calcium-independent phospholipase A2 suppresses proliferation and tumorigenicity of ovarian carcinoma cells, Biochem. J. 406 (2007) 427–436.
[14] M.T. Duvernay, C.M. Filipeanu, G. Wu, The regulatory mechanisms of export trafficking of G protein-coupled receptor, Cell. Signal. 17 (2005) 1457–1465.
[15] T.D. Werry, G.F. Wilkinson, G.B. Willars, Mechanisms of cross-talk between G-protein-coupled receptors resulting in enhanced release of intracellular Ca^{2+}, Biochem. J. 374 (2003) 281–296.
[16] G.V. Glinsky, Apoptosis in metastatic cancer cells, Crit. Rev. Oncol. Hematol. 25 (1997) 175–186.
[17] M.O. Hengartner, The biochemistry of apoptosis, Nature 407 (2000) 770–776.
[18] A. Saraste, K. Pulkki, Morphologic and biochemical hallmarks of apoptosis, Cardiovasc. Res. 45 (2000) 528–537.
[19] D.R. Green, J.C. Reed, Mitochondria and apoptosis, Science 281 (1998) 1309–1312.
[20] J. Jordan, P.W. de Groot, M.F. Galindo, Mitochondria: the headquarters in ischemia-induced neuronal death, Cent. Nerv. Syst. Agents Med. Chem. 11 (2011) 98–106.
[21] F. Chen, T. Wang, Y.F. Wu, Y. Gu, X.L. Xu, S. Zheng, X. Hu, Honokiol: a potent chemotherapy candidate for human colorectal carcinoma, World J. Gastroenterol. 10 (2004) 3459–3463.
[22] K. Ishitsuka, T. Hideshima, M. Hamasaki, N. Raje, S. Kumar, H. Hideshima, N. Shiraishi, H. Yasui, A.M. Roccaro, P. Richardson, K. Podar, S. Le Gouill, D. Chauhan, K. Tamura, J. Arbiser, K.C. Anderson, Honokiol overcomes conventional drug resistance in human multiple myeloma by induction of caspase-dependent and -independent apoptosis, Blood 106 (2005) 1794–1800.
[23] D.S. Ziegler, R.D. Wright, S. Kesari, M.E. Lemieux, M.A. Tran, M. Jain, L. Zawel, A.L. Kung, Resistance of human glioblastoma multiforme cells to growth factor inhibitors is overcome by blockade of inhibitor of apoptosis proteins, J. Clin. Invest. 118 (2008) 3109–3122.
[24] C.A. Kruse, D.H. Mitchell, B.K. Kleinschmidt-DeMasters, W.A. Franklin, H.G. Morse, E.B. Spector, K.O. Lillehei, Characterization of a continuous human glioma cell line DBTRG-05MG: growth kinetics, karyotype, receptor expression, and tumor suppressor gene analyses, In Vitro Cell. Dev. Biol. 28A (1992) 609–614.
[25] G. Grynkiewicz, M. Poenie, R.Y. Tsien, A new generation of Ca indicators with greatly improved fluorescence properties, J. Biol. Chem. 260 (1985) 3440–3450.
[26] J.E. Merritt, R. Jacob, T.J. Hallam, Use of manganese to discriminate between calcium influx and mobilization from internal stores in stimulated human neutrophils, J. Biol. Chem. 264 (1989) 1522–1527.
[27] G. Rothe, G. Valet, Flow cytometric analysis of respiratory burst activity in phagocytes with hydroethidine and 2′,7′-dichlorofluorescin, J. Leukoc. Biol. 47 (1990) 440–448.
[28] D.E. Clapham, Intracellular calcium. Replenishing the stores, Nature 375 (1995) 634–635.
[29] O. Thastrup, P.J. Cullen, B.K. Drøbak, M.R. Hanley, A.P. Dawson, Thapsigargin, a tumor promoter, discharges intracellular Ca^{2+} stores by specific inhibition of the endoplasmic reticulum Ca^{2+}-ATPase, Proc. Natl. Acad. Sci. U.S.A. 87 (1990) 2466–2470.
[30] G.J. Van Esch, Toxicology of tert-butylhydroquinone (TBHQ), Food Chem. Toxicol. 24 (1986) 1063–1065.
[31] M.D. Bootman, P. Lipp, M.J. Berridge, The organisation and functions of local Ca^{2+} signals, J. Cell Sci. 114 (2001) 2213–2222.
[32] T. Takenouchi, K. Ogihara, M. Sato, H. Kitani, Inhibitory effects of U73122 and U73343 on Ca^{2+} influx and pore formation induced by the activation of P2X7 nucleotide receptors in mouse microglial cell line, Biochim. Biophys. Acta 1726 (2005) 177–186.
[33] G. James, A.M. Butt, P2Y and P2X purinoceptor mediated Ca^{2+} signalling in glial cell pathology in the central nervous system, Eur. J. Pharmacol. 447 (2002) 247–260.
[34] R.Y. Tsien, New calcium indicators and buffers with high selectivity against magnesium and protons: design, synthesis, and properties of prototype structures, Biochemistry 19 (1980) 2396–2404.
[35] L.L. Han, L.P. Xie, L.H. Li, X.W. Zhang, R.Q. Zhang, H.Z. Wang, Reactive oxygen species production and Bax/Bcl-2 regulation in honokiol-induced apoptosis in human hepatocellular carcinoma SMMC-7721 cells, Environ. Toxicol. Pharmacol. 28 (2009) 97–103.
[36] G.R. Monteith, D. McAndrew, H.M. Faddy, S.J. Roberts-Thomson, Calcium and cancer: targeting Ca^{2+} transport, Nat. Rev. Cancer 7 (2007) 519–530.
[37] T. Ducret, S. Boudina, B. Sorin, A.M. Vacher, I. Gourdou, D. Liguoro, J. Guerin, L. Bresson-Bepoldin, P. Vacher, Effects of prolactin on intracellular calcium concentration and cell proliferation in human glioma cells, Glia 8 (2002) 200–214.
[38] G.G. Kovacs, A. Zsembery, S.J. Anderson, P. Komlosi, G.Y. Gillespie, P.D. Bell, D.J. Benos, C.M. Fuller, Changes in intracellular Ca^{2+} and pH in response to thapsigargin in human glioblastoma cells and normal astrocytes, Am. J. Physiol. Cell Physiol. 289 (2005) C361–C371.
[39] K.H. Chang, M.D. Yan, C.J. Yao, P.C. Lin, G.M. Lai, Honokiol-induced apoptosis and autophagy in glioblastoma multiforme cells, Oncol. Lett. 6 (2013) 1435–1438.
[40] H. Liu, J.D. Hughes, S. Rollins, B. Chen, E. Perkins, Calcium entry via ORAI1 regulates glioblastoma cell proliferation and apoptosis, Exp. Mol. Pathol. 91 (2011) 753–760.
[41] A. Denys, V. Aires, A. Hichami, N.A. Khan, Thapsigargin-stimulated MAP kinase phosphorylation via CRAC channels and PLD activation: inhibitory action of docosahexaenoic acid, FEBS Lett. 564 (2004) 177–182.
[42] J. Fodor, C. Matta, T. Oláh, T. Juhász, R. Takács, A. Tóth, B. Dienes, L. Csernoch, R. Zákány, Store-operated calcium entry and calcium influx via voltage-operated calcium channels regulate intracellular calcium oscillations in chondrogenic cells, Cell Calcium 54 (2013) 1–16.
[43] N. Jiang, Z.M. Zhang, L. Liu, C. Zhang, Y.L. Zhang, Z.C. Zhang, Effects of Ca^{2+} channel blockers on store-operated Ca^{2+} channel currents of Kupffer cells after hepatic ischemia/reperfusion injury in rats, World J. Gastroenterol. 12 (2006) 4694–4698.
[44] K. Morita, A. Sakakibara, S. Kitayama, K. Kumagai, K. Tanne, T. Dohi, Pituitary adenylate cyclase-activating polypeptide induces a sustained increase in intracellular free Ca^{2+} concentration and catechol amine release by activating Ca^{2+} influx via receptor-stimulated Ca^{2+} entry, independent of store-operated Ca^{2+} channels, and voltage-dependent Ca^{2+} channels in bovine adrenal medullary chromaffin cells, J. Pharmacol. Exp. Ther. 302 (2002) 972–982.
[45] J. Hartmann, A. Verkhratsky, Relations between intracellular Ca^{2+} stores and store-operated Ca^{2+} entry in primary cultured human glioblastoma cells, J. Physiol. 513 (1998) 411–424.
[46] R. Wondergem, T.W. Ecay, F. Mahieu, G. Owsianik, B. Nilius, HGF/SF and menthol increase human glioblastoma cell calcium and migration, Biochem. Biophys. Res. Commun. 372 (2008) 210–215.

[47] A.K. Vogt-Eisele, K. Weber, M.A. Sherkheli, G. Vielhaber, J. Panten, G. Gisselmann, H. Hatt, Monoterpenoid agonists of TRPV3, Br. J. Pharmacol. 151 (2007) 530–540.
[48] M. Kang, H.G. Othmer, The variety of cytosolic calcium responses and possible roles of PLC and PKC, Phys. Biol. 4 (2007) 325–343.
[49] R.C. Soletti, T. Alves, J. Vernal, H. Terenzi, G. Anderluh, H.L. Borges, N.H. Gabilan, V. Moura-Neto, Inhibition of MAPK/ERK, PKC and CaMKII signaling blocks cytolysin-induced human glioma cell death, Anticancer Res. 30 (2010) 1209–1215.
[50] Z. Li, Y. Liu, X. Zhao, X. Pan, R. Yin, C. Huang, L. Chen, Y. Wei, Honokiol, a natural therapeutic candidate, induces apoptosis and inhibits angiogenesis of ovarian tumor cells, Eur. J. Obstet. Gynecol. Reprod. Biol. 140 (2008) 95–102.
[51] D.E. Clapham, Calcium signaling, Cell 131 (2007) 1047–1058.
[52] J. Matuszyk, M. Kobzdej, E. Ziolo, W. Kalas, P. Kisielow, L. Strzadala, Thymic lymphomas are resistant to Nur77-mediated apoptosis, Biochem. Biophys. Res. Commun. 249 (1998) 279–282.
[53] T.M. Nicotera, D.P. Schuster, M. Bourhim, K. Chadha, G. Klaich, D.A. Corral, Regulation of PSA secretion and survival signaling by calcium-independent phospholipase A(2) beta in prostate cancer cells, Prostate 69 (2009) 1270–1280.
[54] G. Simbula, A. Columbano, G.M. Ledda-Columbano, L. Sanna, M. Deidda, A. Diana, M. Pibiri, Increased ROS generation and p53 activation in alpha-lipoic acid-induced apoptosis of hepatoma cells, Apoptosis 12 (2007) 113–123.
[55] J.W. Lin, J.T. Chen, C.Y. Hong, Y.L. Lin, K.T. Wang, C.J. Yao, G.M. Lai, R.M. Chen, Honokiol traverses the blood–brain barrier and induces apoptosis of neuroblastoma cells via an intrinsic bax–mitochondrion–cytochrome c–caspase protease pathway, Neuro. Oncol. 14 (2012) 302–314.
[56] X. Wang, X. Duan, G. Yang, X. Zhang, L. Deng, H. Zheng, C. Deng, J. Wen, N. Wang, C. Peng, X. Zhao, Y. Wei, L. Chen, Honokiol crosses BBB and BCSFB, and inhibits brain tumor growth in rat 9 L intracerebral gliosarcoma model and human U251 xenograft glioma model, PLoS ONE 6 (2011) e18490.
[57] A.J. Lin, S.H. Wang, K.C. Chen, H.P. Kuei, Y.L. Shih, S.Y. Hou, W.T. Chiu, S.H. Hsiao, C.M. Shih, Evodiamine, a plant alkaloid, induces calcium/JNK-mediated autophagy and calcium/mitochondria-mediated apoptosis in human glioblastoma cells, Chem. Biol. Interact. 205 (2013) 20–28.